Inorganic Chemistry

Article

pubs.acs.org/IC

Intramolecular Direct Oxygen Transfer from Oxoferryl Porphyrin to a Sulfide Bond

Takunori Ueda, Hiroaki Kitagishi, and Koji Kano*

Department of Molecular Chemistry and Biochemistry, Doshisha University, Kyotanabe, Kyoto 610-0321, Japan

Supporting Information

ABSTRACT: A 1:1 supramolecular complex (met-hemoCD) of 5,10,15,20-tetrakis(4-sulfonatophenyl)porphyrinatoiron(III) (Fe^{III}TPPS) with a per-*O*-methylated β-cyclodextrin dimer having a $-SCH_2PyCH_2S-$ (Py = pyridin-3,5-diyl) linker (Py3CD) reacted rapidly with hydrogen peroxide or cumene hydroperoxide in an aqueous solution forming two types of hydroperoxo or alkylperoxo intermediates, ROO-Fe^{III}(OH^-)PCD and ROO-Fe^{III}(Py)PCD, which underwent rapid homolysis to the corresponding ferryloxo species, namely, O=Fe^{IV}(OH^-)PCD and O=Fe^{IV}(Py)PCD, respectively. For the O=Fe^{IV}(OH^-)PCD species, the iron-oxo oxygen facing the linker gradually transferred to the nearby sulfide bond on the linker, forming the sulfoxidized Py3CD (Py3CD-O)/Fe^{II}TPPS complex, which then bound dioxygen in air forming an oxy-ferrous complex, O_2-Fe^{II}TPPS/Py3CD-O. In contrast, the O=Fe^{IV}(Py)PCD species, in which the iron-oxo oxygen was located on the opposite side of the sulfide bond on the linker across the porphyrin ring, was reduced to the resting state (met-hemoCD) by the surroundings without any oxidation of the Py3CD linker.

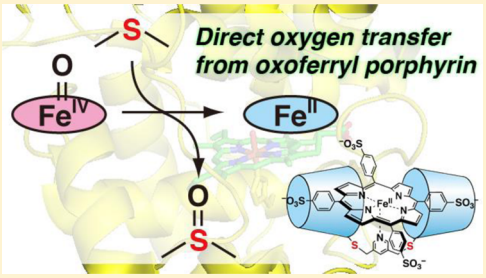

INTRODUCTION

The redox reactions catalyzed by heme enzymes are a fascinating subject for chemists, because of the diverse heme-catalyzed reactions with complicated reaction mechanisms, even though heme or hemin is the common prosthetic group of such enzymes.[1] Cytochrome P450 (Cyt P450) and horseradish peroxidase (HRP) utilize molecular oxygen and hydrogen peroxide (H_2O_2), respectively, as the primary oxidants. Different axial ligands and environments around the porphyrin center in these two enzymes have been assumed to be responsible for the dissimilarities between the enzymatic activities.[2] Both the enzymatic reactions have common reaction intermediates such as an oxoferryl porphyrin cation radical, Cpd I, which is the highly active intermediate in heme-catalyzed oxidation reactions. Although the hydroxylation of alkanes and epoxidation of alkenes by Cpd I are well-known enzymatic reactions, their exact reaction mechanisms have yet to be established.[3] The dealkylation of *N*-alkylamines and sulfoxidation of sulfides are convenient probes to study the Cpd I-catalyzed oxidation mechanisms. Three types of mechanisms are proposed for Cpd I-catalyzed oxidation: (1) an electron-transfer (ET) from the substrate to a Cpd I intermediate yielding a Cpd II intermediate, an oxoferryl porphyrin, and the cation radical of the substrate, followed by the oxygen rebound (OR) from the Cpd II intermediate to the cation radical of the substrate (ET-OR mechanism, two one-electron oxidations); (2) direct oxygen transfer (DOT) from a Cpd I intermediate to the substrate yielding the ferric porphyrin resting state and the oxygenated substrate (DOT mechanism, two-electron oxidation); and (3) hydrogen or proton−electron transfer (HT/PET) from the substrate to a Cpd I intermediate followed by the oxygen uptake of the resulting substrate radical (HT/PET mechanism). Watanabe and co-workers reported that the sulfoxidation of thioanisole catalyzed by the Cpd I intermediate of HRP proceeds through a one-electron transfer process from the thioanisole to the Cpd I intermediate, yielding a thioanisole cation radical and the corresponding oxoferryl porphyrin (Cpd II), followed by an oxygen transfer (25%) from the Cpd II intermediate to the thioanisole cation radical in a protein cage.[4] The ET/OR mechanism for the sulfoxidation by the Cpd I intermediates of HRP has been well established.[2,5] The same ET/OR mechanism has been proposed for the sulfoxidation of thioanisole by Cyt P450.[6] However, there is a controversy over the sulfoxidation mechanism by the Cpd I intermediate of Cyt P450. Recently, the calculations strongly support the existence of a DOT mechanism, even though the sulfoxidation rates agree well with the oxidation potentials of thioether substrates.[7] There is no experimental evidence for establishing the DOT mechanism for sulfoxidation by the Cpd I intermediates of Cyt P450, while the sulfoxidations of thioanisoles by the Cpd I intermediates of chloroperoxidase (CPO),[8] heme oxygenase,[9] a myoglobin mutant,[4] and a reconstituted HRP[10] have been demonstrated to occur through the DOT mechanism.[8,9] The *N*-oxidation of alkyl amines by the Cpd I intermediates of Cyt P450 was reported to proceed through the DOT mechanism.[11] Although the HT mechanism has been proposed for the Cpd I-catalyzed oxygenation of alkanes,[3b,12] this mechanism is excluded for the sulfoxidation reaction.

Received: October 21, 2013
Published: December 12, 2013

Scheme 1

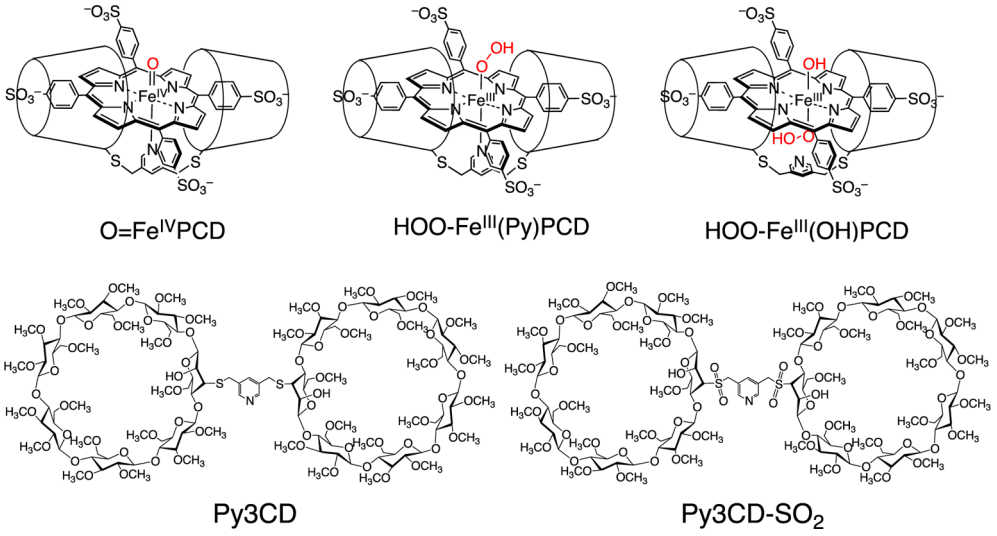

In contrast to Cpd I intermediates, there are few studies on the reactivity of Cpd II intermediates. In the HRP (Cpd I)-catalyzed oxidation of alkanes/alkenes, the oxygen atom introduced into the alkyl group or C=C double bond of the substrate originates from either O_2 or H_2O molecule.[12] To the best of our knowledge, no example has been shown of a direct oxygen transfer from the biological Cpd II intermediates to an alkane/alkene. In general, the reactivity of Cpd II intermediate is much lower than that of Cpd I intermediate. The difficulties in preparing pure Cpd II intermediate make it difficult to study the reactions of Cpd II intermediate in detail.

Unlike in the case of biological heme enzymes, there are few reports on the preparation and the reactions of Cpd I-type species in model systems.[13−17] In contrast, the Cpd II-type oxoferryl porphyrins show diverse reactivity. The reaction of triphenylphosphine with dioxygen in toluene catalyzed by Fe^{II}TPP (TPP = meso-tetraphenylporphyrin dianion) yielding triphenylphosphine oxide has been assumed to proceed through O=Fe^{IV}TPP species.[18] The treatment of $Fe^{III}TMP^{\bullet+}(ClO_4)_2$ (TMP = meso-tetramesitylporphyrin dianion) with basic alumina in CH_2Cl_2 or benzene containing H_2O afforded O=Fe^{IV}TMP species, which then reacted with styrene to yield styrene oxide and benzaldehyde via a $C_6H_5CH(\bullet)CH_2O-Fe^{III}$TMP radical intermediate.[19] More convenient methods for preparation of Cpd II-type oxoferryl porphyrins have been developed, and their reactions such as epoxidation,[20] hydroxylation,[20] dealkylation,[21] and oxidation of dihydroaromatics[22,23] have been investigated. It has been assumed that O=$Fe^{IV}TPFPP^{\bullet+}$, which is formed by the disproportionation of O=Fe^{IV}TPFPP species in an organic solvent containing H_2O, is the actual reactive species in the oxidation reactions catalyzed by O=Fe^{IV}TPFPP,[24] even though there is controversy on this topic.[21]

Despite these studies, because of diverse reaction conditions employed and no established methods to prepare pure oxoferryl porphyrin cation radicals and oxoferryl porphyrins, some aspects of heme enzyme models are still unclear. Most of the model systems have been studied using iron porphyrins in the absence of axial ligands in organic solvents with excess amounts of strong primary oxidants such as H_2O_2, *m*-chloroperbenzoic acid (mCPBA), and iodosylbenzene. For example, excess H_2O_2 is known to react with the Cpd II intermediate of HRP yielding Cpd III ($\bullet O_2-Fe^{III}$).[25] The laboratory reactions employed for the heme enzyme models are far from those of a biological system. Therefore, to study the reactivity of synthetic oxoferryl intermediates as Cpd I and II chemical models, their reactions should be examined by using pure oxoferryl intermediates in an aqueous solution without excess primary oxidants. Moreover, it is better to design a model system in which the iron porphyrin is coordinated by a fifth axial ligand.

The introduction of supramolecular chemistry into the model systems for heme-catalyzed oxidation has been rarely explored. One of the few examples involves the formation of an oxoferryl porphyrin by the reaction of H_2O_2 with Fe^{III}TPPS (TPPS = meso-tetrakis(4-sulfonatophenyl)porphyrin hexa-anion), which is encapsulated by a per-*O*-methylated *β*-cyclodextrin dimer (Py3CD, Scheme 1) with a $-SCH_2PyCH_2S-$ (Py = pyridin-3,5-diyl) linker, in an aqueous solution.[26] The 1:1 inclusion complex of Fe^{III}TPPS with Py3CD has been named as met-hemoCD,[27] in which the sixth axial ligand is OH^- at pH 7.0 (pK_a of H_2O-Fe^{III}TPPS/Py3CD = 5.5).[28] The reaction of Fe^{III}TPPS with H_2O_2 in the presence of a supramolecular host, Py3CD, affords O=Fe^{IV}TPPS/Py3CD complex (abbreviated as O=Fe^{IV}PCD, Scheme 1) without appreciable byproducts, whereas no oxoferryl porphyrin was obtained in the reaction of uncomplexed Fe^{III}TPPS (without Py3CD) with H_2O_2.[29] In the absence of Py3CD, rapid ring-opening reactions of Fe^{III}TPPS occurred. Such an all-or-nothing reaction has not been understood completely. Py3CD may act as an artificial substitute for apoenzymes. In the present study, we tried to better understand the reaction of met-hemoCD (HO-Fe^{III}PCD) with H_2O_2. We mainly focused on (1) the effects of Py3CD on the stabilization of O=Fe^{IV}PCD species and (2) the fate of iron-oxo oxygen of O=Fe^{IV}PCD. Py3CD contains two sulfide bonds at the linker position, which may act as the receptor of the iron-oxo oxygen of O=Fe^{IV}PCD species. In this study, O=Fe^{IV}PCD species was protected from excess oxidant, and all the reactions were carried out in aqueous solutions. Therefore, the present supramolecular system can be claimed as a unique and advanced heme enzyme model.

dx.doi.org/10.1021/ic4026393 | *Inorg. Chem.* 2014, 53, 543−551

EXPERIMENTAL SECTION

Materials. $Fe^{III}TPPS$[30] and Py3CD[27] were prepared and purified according to the procedures described in the literature. Fe^{III}P-PEG5K (molecular weight of polyethylene glycol = ca. 5000) was the same as before.[31] The concentrations of hydrogen peroxide and cumene hydroperoxide (CHPO) were determined based on their iodometry before use. $^{18}O_2$ (99 atom %) was purchased from ISOTEC. ^{18}O-labeled CHPO ($R^{18}O-{}^{18}OH$, 90 atom %) was synthesized according to the procedure described in the literature.[32]

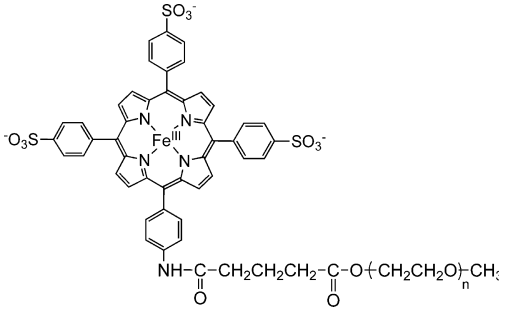

Fe^{III}P-PEG5K

Instruments. UV−vis spectra were recorded on a Shimadzu MultiSpec-1500 photodiode-array spectrometer with a thermostatic cell holder. The ^1H NMR spectra were taken on a JEOL JNM-ECA 500. EPR measurements were made using a JEOL JES-TE200 spectrometer (X-band) at room temperature using a quartz flat cell and at 77 K using an EPR tube. The simulated EPR spectrum was obtained using the ISOTROPIC SIMULATION ver. 2.1 (JEOL) program. The ESI-TOF mass spectra were taken on a JEOL JMS-T100CS spectrometer. MALDI-TOF mass spectra were recorded on a Bruker Daltonics autoflex speed spectrometer. The mass scale was calibrated based on heptakis(2,3,6-tri-*O*-methyl)-*β*-cyclodextrin ($[M + Na]^+$, m/z = 1451.68, Nakalai). A HPLC analysis was performed using a Wakosil-II 5C18AR column (4.6 × 250 mm, reverse-phase silica gel, Wako) attached to a GE Healthcare ÄKTA purifier HPLC system.

Preparation of O=Fe^{IV}PCD Solution. An excess amount of CHPO (20 equiv) was added to 0.2 mL of a met-hemoCD solution ($[Fe^{III}TPPS] = [Py3CD]$ = 0.5 mM in a 0.05 M phosphate buffer at pH 7.0). After ca. 10 s, the resulting solution was charged to a Sephadex G-25 column (HiTrap desalting column, GE Healthcare) and eluted with the phosphate buffer solution to remove excess CHPO and its decomposed products. The purified O=Fe^{IV}PCD solution (1 mL) was used immediately. The concentration of O=Fe^{IV}PCD was determined using the extinction coefficient at 422 nm (ε_{max} = 1.55 × 10^5 M^{-1} cm^{-1}).

Postreaction Analysis of the Cyclodextrin Dimer. After the reaction of met-hemoCD with hydrogen peroxide or CHPO, the reaction mixture was extracted using $CHCl_3$. The organic layer was concentrated and the residue was analyzed through ESI-TOF MS. To prepare a sample for the ESI-TOF MS analysis, the cyclodextrin extract was dissolved in a MeOH/H_2O (1:1) solution containing 0.1 mM sodium acetate followed by filtration with a syringe filter (0.45 μm hydrophilic cellulose acetate, DISMIC-25CS, Advantec). To prepare a sample for HPLC analysis, a $CHCl_3$ extract of cyclodextrin components was dissolved in water and filtered with a syringe filter (0.45 μm hydrophilic cellulose acetate, DISMIC-25CS, Advantec).

Disulfonylation of Py3CD. Py3CD (100 mg, 34 μmol) was dissolved in a 1:1 mixture of water and methanol (20 mL) in a 50 mL round-bottom flask, and the mixture was cooled in an ice bath. Oxone (124 mg, 0.2 mmol) was added into the flask, and the mixture was stirred for 30 min at room temperature. Water (10 mL) was added to the reaction mixture and extracted using dichloromethane (30 mL × 3), and the combined organic layer was dried on anhydrous Na_2SO_4. The solvent of the organic layer was evaporated, generating crude disulfonylated Py3CD (Py3CD-SO_2, Scheme 1). GPC (JAIGEL GS-310) with methanol gave a colorless solid (83 mg, 81%). ^1H NMR (500 MHz, $CDCl_3$): δ 8.76 (s, 2H), 8.09 (s, 1H), 5.41−5.07 (m, 14H), 4.80−3.20 (m, 206). MS (MALDI-TOF, α-cyano-4-hydroxycinnamic acid) m/z: calcd for $[M + Na]^+$ 3023.3; found 3023.3. Elemental analysis (%) for $C_{129}H_{221}NO_{72}S_2{\cdot}5H_2O$: C, 50.10; H, 7.53; N, 0.45; found: C, 49.93; H, 7.26; N, 0.53.

RESULTS AND DISCUSSION

Formation of O=Fe^{IV}PCD. The addition of H_2O_2 (2×10^{-4} M) into a 1:1 complex of $Fe^{III}TPPS$ and Py3CD (abbreviated as met-hemoCD, $[Fe^{III}TPPS] = 1 \times 10^{-5}$ M, $[Py3CD] = 1.2 \times 10^{-5}$ M) in a 0.05 M phosphate buffer at pH 7.0 caused shifts in the absorption maxima from 418 and 571 nm owing to met-hemoCD to 422 and 558 nm owing to the oxoferryl complex (O=Fe^{IV}PCD).[26] The pseudo-first-order rate constant (k_{obs}) for the formation of O=Fe^{IV}PCD was 0.011 s^{-1} at 25 °C (Figure S1, Supporting Information). Increases in both the concentrations of met-hemoCD and H_2O_2 dramatically accelerated the formation of O=Fe^{IV}PCD (k_{obs} = 0.098 s^{-1} at $[met\text{-}hemoCD] = 5 \times 10^{-4}$ M, $[H_2O_2] = 5 \times 10^{-3}$ M). The second-order rate constant for the formation of O=Fe^{IV}PCD could not be accurately determined, because a decomposition of O=Fe^{IV}PCD occurred competitively at higher concentrations of H_2O_2. We hypothesize that the generation of hydroxyl radicals in the reaction of O=Fe^{IV}PCD with excess H_2O_2 affording HOO-Fe^{III}PCD[26] is responsible for the decomposition of O=Fe^{IV}PCD. CHPO was used in place of H_2O_2 because CHPO does not generate a hydroxyl radical. The UV−vis spectral changes during the reaction of met-hemoCD with CHPO are shown in Figure 1. Although the

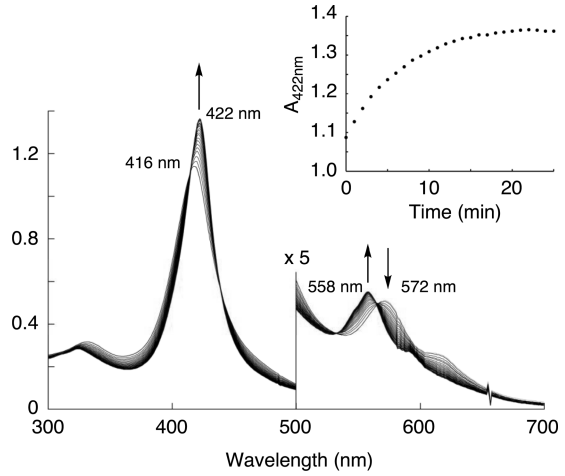

Figure 1. UV−vis spectral changes during the reaction of met-hemoCD ($[Fe^{III}TPPS] = 1 \times 10^{-5}$ M, $[Py3CD] = 1.2 \times 10^{-5}$ M) with CHPO (2.0×10^{-4} M) in 0.05 M phosphate buffer at pH 7.0 and 25 °C. Spectra were recorded at time intervals of 1 min. The inset is the progressive absorbance change at 422 nm.

isosbestic point at around 569 nm slightly moved to shorter wavelength as the reaction proceeded, no marked decomposition of O=Fe^{IV}PCD was observed. The extinction coefficients of O=Fe^{IV}PCD were tentatively determined to be 1.55 × 10^5 M^{-1} cm^{-1} at 422 nm and 1.21 × 10^4 M^{-1} cm^{-1} at 558 nm. In the absence of Py3CD, a μ-oxo dimer of $Fe^{III}TPPS$ decomposed after the addition of H_2O_2 or CHPO (Figure S2, Supporting Information). In particular, the reaction with H_2O_2 caused a rapid decomposition of FeTPPS.[26] In the presence of Py3CD, however, no marked decomposition of met-hemoCD occurred at a lower H_2O_2 concentration, and the yield of O=

dx.doi.org/10.1021/ic4026393 | Inorg. Chem. 2014, 53, 543−551

Fe^{IV}PCD was 86% in the reaction of met-hemoCD (1×10^{-5} M) with H_2O_2 (2×10^{-4} M). The rapid decomposition of FeTPPS in the reaction with H_2O_2 seems to be ascribed to the generation of very active hydroxyl radical during the reaction.[33] We assumed that the hydroxyl radicals were deactivated by Py3CD. To verify this assumption, it was essential to detect the generation of hydroxyl radicals during the reaction of met-hemoCD with H_2O_2. 5,5-Dimethyl-1-pyrroline-*N*-oxide (DMPO) was used as a spin-trap reagent. The EPR spectrum of the trapped species is shown in Figure 2. The trapped

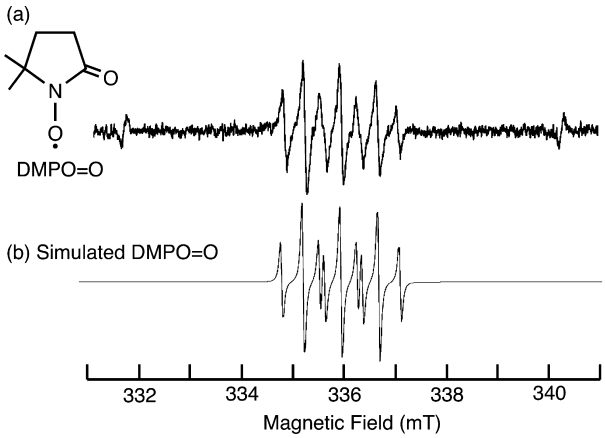

Figure 2. EPR spectrum measured in the reaction of met-hemoCD ([Fe^{III}TPPS] = [Py3CD] = 2×10^{-3} M) with H_2O_2 (1×10^{-2} M) in 0.05 M phosphate buffer (pH 7.0) containing DMPO (5×10^{-4} M) at 25 °C (a) and the computer-simulated spectrum of DMPO═O (a_H = 0.41 T, a_N = 0.72 T) (b). The spectrum was recorded 1 min after mixing of met-hemoCD, H_2O_2, and DMPO. Microwave power: 1.0 mW, modulation width: 50 μT, time constant: 0.03 s.

radicals were not DMPO-OH but rather DMPO═O, which is an oxidized product of DMPO-OH (see eq 1).[34] Because

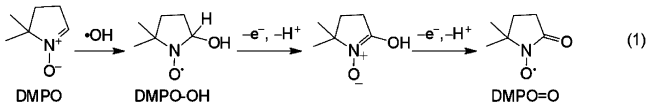

(1)

DMPO-OH is plausibly oxidized by simultaneously formed O═Fe^{IV}PCD (eq 1), the EPR result strongly supports the homolysis of HOO-Fe^{III}PCD (Cpd 0 mimic) yielding hydroxyl radicals and O═Fe^{IV}PCD. In the absence of Py3CD, the reaction of the μ-oxo-dimer of Fe^{III}TPPS with H_2O_2 yielded various ring-opening products, the formations of which were analyzed using HPLC and MADI-TOF MS (Figure S3, Supporting Information). The ring-opening reactions were assumed to be initiated by an attack of an •OH radical at a meso-position of the porphyrin. Such a reaction was strictly inhibited by Py3CD, which contains the per-*O*-methylated glucopyranose units and sulfide bonds as radical scavenger candidates. The transformation of Py3CD after the formation of O═Fe^{IV}PCD was then analyzed. Hydrogen peroxide (5×10^{-3} M) was added into an equimolar mixture of Fe^{III}TPPS and Py3CD (5×10^{-4} M) in a pH 7.0 phosphate buffer at 25 °C. After 30 s, the reaction mixture was extracted by $CHCl_3$, and the extract was analyzed using ESI-TOF MS. The result is shown in Figure 3. The main peak was observed at *m*/*z* 2959 ($[M + Na]^+$) owing to the Py3CD itself along with a weak peak at *m*/*z* 2975 ($[M + 16 + Na]^+$). Although the UV−vis spectrum indicated a complete conversion of met-hemoCD into O═

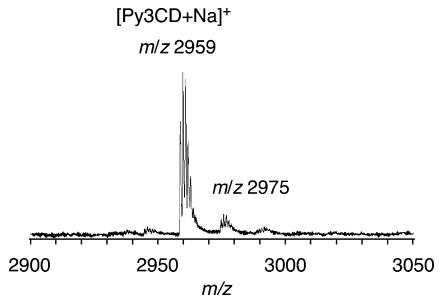

Figure 3. ESI-TOF mass spectrum of the $CHCl_3$ extract of the mixture obtained by reacting met-hemoCD ([Fe^{III}TPPS] = [Py3CD] = 5×10^{-4} M) with H_2O_2 (5×10^{-3} M) in 0.05 M phosphate buffer at pH 7.0 for 30 s.

Fe^{IV}PCD, no marked transformation of Py3CD was observed at the instant of complete conversion of met-hemoCD into O═Fe^{IV}PCD. The only process explaining the inactivation of the hydroxyl radical is a coupling of the •OH radicals affording less active H_2O_2. It is known that Py3CD, including a $TPPSH_2$ free base or its iron complex, constructs a tight and hydrophobic capsule.[27,30] The formation of O═Fe^{IV}PCD in a Py3CD capsule is represented as Scheme 2. It seems that the hydroxyl

Scheme 2

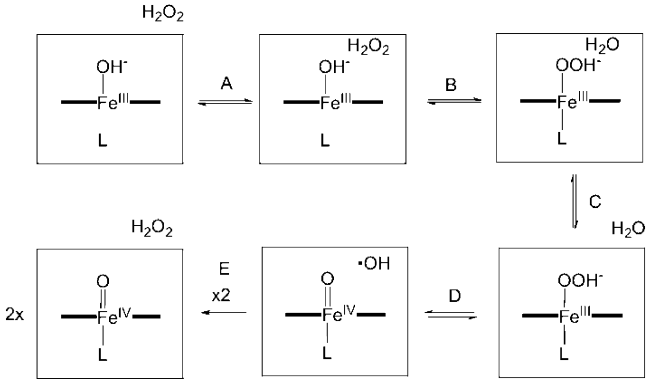

radical in the capsule is stabilized by equilibrium D in Scheme 2. A highly active hydroxyl radical may predominantly exist in the form of HOO-Fe^{III}PCD in the cyclodextrin capsule (equilibrium D), which immediately reacts with other HOO-Fe^{III}PCD to produce an H_2O_2 molecule and two O═Fe^{IV}PCD molecules when two capsules collide with each other (process E).

If our hypothesis is correct, HOO-Fe^{III}PCD should be stabilized when the collision between the two cyclodextrin capsules is inhibited. Then we used Fe^{III}P-PEG5K in place of Fe^{III}TPPS, because a long polyethylene glycol (PEG) chain may inhibit the collision between the cyclodextrin capsules. The effect of the PEG chain on the stabilization of the hydroperoxo complex of Fe^{III}P-PEG5K complexed with Py3CD was evaluated by EPR spectra. As reported previously, two sets of the rhombic signals owing to HOO-Fe^{III}PCD were observed when the sample was frozen at 15 K immediately after met-hemoCD and H_2O_2 were mixed.[26] In this study, the measurements were carried out at 77 K. The EPR spectra were measured at appropriate waiting times until freezing the sample prepared by mixing Fe^{III}P-PEG5K (5×10^{-4} M), Py3CD (7.5×10^{-5} M), and H_2O_2 (2.5×10^{-3} M). The results are shown in Figure 4a, together with the EPR spectra of the

dx.doi.org/10.1021/ic4026393 | *Inorg. Chem.* 2014, 53, 543−551

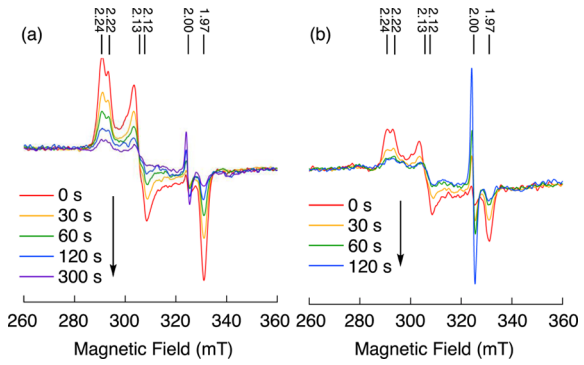

Figure 4. EPR spectra of the reaction mixtures of H_2O_2 (2.5×10^{-3} M) with Fe^{III}P-PEG5K (5×10^{-4} M) complexed with Py3CD (7.5×10^{-4} M) (a) and met-hemoCD (5×10^{-4} M) (b) in 0.05 M phosphate buffer at pH 7.0 and 77 K. The solutions were frozen by liquid N_2 at the appropriate times after mixing H_2O_2.

mixture of met-hemoCD and H_2O_2 for reference (Figure 4b). In accord with the previous result, two sets of the signals due to the two low-spin states were observed in both cases of FeTPPS and the PEGylated iron porphyrin incorporated in the Py3CD capsules. The rhombic signals from met-hemoCD were assigned to two types of HOO-Fe^{III}PCDs whose iron centers were coordinated by the pyridine moiety at the linker position (HOO-Fe^{III}(Py)PCD) and the OH^- anion (HOO-Fe^{III}(OH^-)-PCD).[26] The intensity of the EPR signals for the Fe^{III}P-PEG5K sample at the waiting time = 0 s was much stronger than those for the met-hemoCD sample. In addition, the hydroperoxo complexes of the PEGylated sample were much more stable than those of the met-hemoCD sample. Because Fe^{III}P-PEG5K has a long PEG chain, the porphyrin sites in the two independent Py3CD capsules may hardly collide with each other due to the steric hindrance. Such a result supports the hypothesis that the hydroxyl radical is stabilized by the equilibrium D in Scheme 2.

Spontaneous Decomposition of O═Fe^{IV}PCD. In the presence of an excess H_2O_2 or CHPO, O═Fe^{IV}PCD gradually decomposed (Figure S1, Supporting Information). To study the reactivity of O═Fe^{IV}PCD itself, excess oxidant should be removed from the reaction system. CHPO (0.01 M) was added into the met-hemoCD solution (5×10^{-4} M) in a phosphate buffer (100 μL). The color of the mixture changed from brown to red within ca. 10 s. Hereafter, the reaction mixture at this moment is called Sample A.

Sample A was passed through a gel-filtration column (HiTrap, GE Healthcare) with a 0.05 M phosphate buffer at pH 7.0 (0.5 mL/min). The chromatogram (Figure S4, Supporting Information) indicated a complete separation of O═Fe^{IV}PCD and CHPO and its derivatives. The concentration of O═Fe^{IV}PCD in an eluted sample was estimated from the absorbance at 422 nm (ε_{max} = 1.55×10^5 M^{-1} cm^{-1}). Hereafter, the freshly separated O═Fe^{IV}PCD solution (1 mL) is called Sample B.

O═Fe^{IV}PCD in an appropriately diluted Sample B spontaneously decomposed to give a product having λ_{max} at 422 and 544 nm (Figure 5a), which is in good agreement with the absorption maxima of the dioxygen adduct of the Fe^{II}PCD complex (O_2-Fe^{II}PCD).[27] Because the cyclodextrin host of this supramolecular dioxygen adduct is not Py3CD as shown later, the dioxygen adduct is abbreviated as O_2-Fe^{II}PCD-O hereafter. After 1 h, the reaction mixture was placed under a CO atmosphere, and the UV−vis spectrum was measured (Figure 5b). A sharp absorption band from the CO-Fe^{II}PCD-O appeared at 422 nm, although the absorbance at 422 nm was too small to conclude that O_2-Fe^{II}PCD-O was the sole reaction product of O═Fe^{IV}PCD. Because the most plausible by-product was met-hemoCD (HO-Fe^{III}PCD), $Na_2S_2O_4$ was added to the reaction mixture under a CO atmosphere to convert the coexisting met-hemoCD into CO-Fe^{II}PCD. This treatment caused a further increase in the absorbance owing to the CO-Fe^{II}PCD (Figure 5b). From the absorbance of the final sample at 422 nm, the total concentration of the FeTPPS/Py3CD complex could be evaluated.[28] Assuming that met-hemoCD is the sole byproduct in the spontaneous reaction of O═Fe^{IV}PCD, the ratio of [O_2-Fe^{II}PCD-O]/[met-hemoCD] in the final reaction mixture was determined to be 49/51. For the calculation, we assumed that the extinction coefficient of CO-

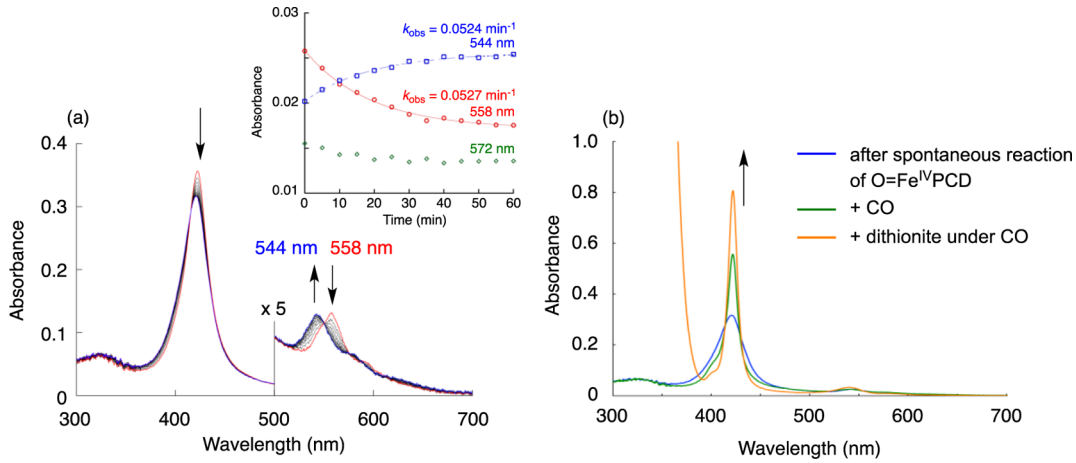

Figure 5. UV−vis spectral changes in the spontaneous reaction of O═Fe^{IV}PCD (2×10^{-6} M) in 0.05 M phosphate buffer at pH 7.0 and 25 °C (a) and UV−vis spectral changes of the reaction mixture of O═Fe^{IV}PCD upon changing the atmosphere from air to CO (b). Spectra in Figure 5a were recorded at time intervals of 5 min. The inset is the progressive changes in absorbances at 542 nm (O_2-Fe^{II}PCD-O), 558 nm (O═Fe^{IV}PCD), and 572 nm (HO-Fe^{III}PCD). The solid lines are the theoretical curves for the first-order kinetics. The green spectrum in panel b was taken after standing the O═Fe^{IV}PCD solution for 1 h and then introducing CO gas into the reaction mixture. The orange spectrum in panel b was measured by adding excess $Na_2S_2O_4$ into the sample showing the green spectrum under a CO atmosphere.

dx.doi.org/10.1021/ic4026393 | Inorg. Chem. 2014, 53, 543−551

Fe^{II}PCD-O is the same as that of CO-Fe^{II}PCD. The reaction products of O=Fe^{IV}PCD under an Ar atmosphere were Fe^{II}PCD-O (λ_{max} = ca. 430 (sh) and 528 nm) and met-hemoCD (λ_{max} = ca. 420 and 572 nm), indicating that the dioxygen of O_2-Fe^{II}PCD-O came from the air. It has been reported that Cpd III (an O_2 adduct of HRP) is formed by a reaction of HRP-Cpd II with H_2O_2.[25,35] In the present system, however, such a route is excluded. The results indicated the occurrence of an intramolecular two-electron redox reaction of O=Fe^{IV}PCD. The transformation of Py3CD after the spontaneous reaction of O=Fe^{IV}PCD was next investigated through ESI-TOF MS.

The host cyclodextrin components in Sample B were extracted by $CHCl_3$, and the ESI-TOF mass spectrum of the extract was measured. The result is shown in Figure 6a. The

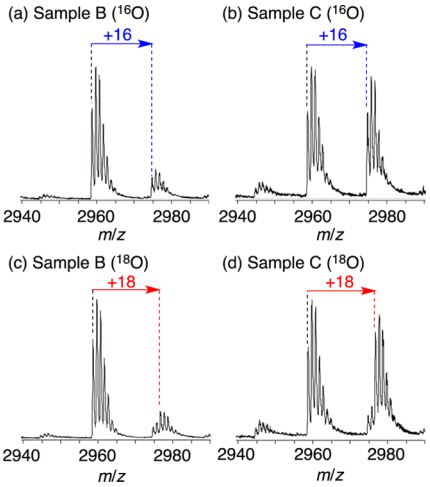

Figure 6. ESI-TOF mass spectra of the $CHCl_3$ extracts of Samples B (a) and C (b) obtained from the reaction of met-hemoCD with ^{16}O-CHPO and those of the corresponding samples (c, d) obtained from the reaction with ^{18}O-CHPO.

peak was observed at m/z 2959 ($[M + Na]^+$), along with small peaks at m/z 2945 and 2975. The result is essentially the same as that for the reaction of met-hemoCD with H_2O_2 (see Figure 3). Enhanced three peaks were observed at m/z 2945 ($[M - 14 + Na]^+$), 2975 ($[M + 16 + Na]^+$), and 2992 ($[M + 32 + Na]^+$) in the $CHCl_3$ extract of Sample C (Figure 6b), which was the reaction mixture obtained by letting Sample B stand for 1 h at room temperature. A prominent peak was observed at m/z 2975, which corresponds to the product formed by the insertion of an oxygen atom into Py3CD. It is impossible to assign the $[M + 16 + Na]^+$ peak to the acetal ($HOCH_2$-O-R), which may be formed by the hydroxylation of the OCH_3 group of per-*O*-methylated glucopyranose of Py3CD. Therefore, the sulfoxidation of Py3CD has to be considered as the major process of the intramolecular reaction of O=Fe^{IV}PCD.

It was difficult to directly prove the formation of a sulfoxide bond. Disulfonylated Py3CD (Py3CD-SO_2, Scheme 1) was next used in place of Py3CD to examine the role of the sulfide bonds in the spontaneous reaction of O=Fe^{IV}PCD. After the reaction of the Fe^{III}TPPS/Py3CD-SO_2 complex ($[Fe^{III}TPPS] = 1.0 \times 10^{-5}$ M, $[Py3CD\text{-}SO_2] = 1.2 \times 10^{-5}$ M) with CHPO (2.0×10^{-4} M) for ca. 10 s, the reaction mixture was passed through a gel-filtration column (HiTrap, GE Healthcare) to separate the O=Fe^{IV}TPPS/Py3CD-SO_2 from the oxidant. The UV–vis spectral changes of O=Fe^{IV}TPPS/Py3CD-SO_2 after the gel-filtration are shown in Figure 7 and are quite different from those for O=Fe^{IV}PCD shown in Figure 5. The spectrum of the

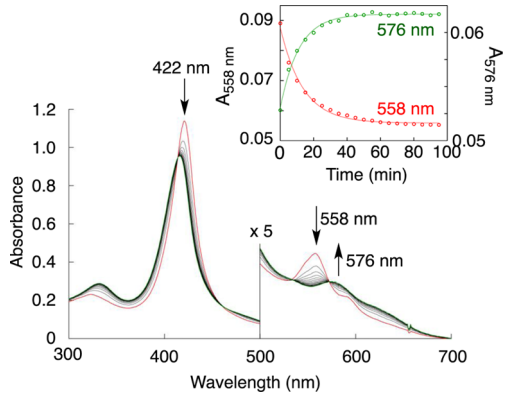

Figure 7. UV–vis spectral changes in spontaneous reaction of the O=Fe^{IV}TPPS/Py3CD-SO_2 complex in 0.05 M phosphate buffer at pH 7.0 and 25 °C. Inset is the progressive changes in absorbances at 558 nm (O=Fe^{IV}TPPS/Py3CD-SO_2) and 576 nm (HO-Fe^{III}TPPS/Py3CD-SO_2).

final product is ascribed to the Fe^{III}TPPS/Py3CD-SO_2 complex and indicates that no dioxygen adduct of the Fe^{II}TPPS/Py3CD-SO_2 complex is formed. The result shows the important role of the sulfide bond in the spontaneous reaction of O=Fe^{IV}PCD affording O_2-Fe^{II}PCD-O.

Sulfoxides and sulfones are known to be reduced to sulfides by magnesium metal in methanol.[36] Such a reaction was applied to verify the sulfoxidation of O=Fe^{IV}PCD. The cyclodextrin components in Sample C were extracted by $CHCl_3$, and the solvent was evapolated from the extract. The residue was dissolved in methanol (1 mL) followed by the addition of magnesium metal (10.2 mg) and iodine crystals (1.2 mg). The mixture was stirred for 2 h at room temperature under an Ar atmosphere. After the reaction, methanol was removed and the residue was extracted by a mixture of $CHCl_3$ and water. The solvent was evaporated from the $CHCl_3$ layer, and the residue was analyzed using MALDI-TOF MS. The result showed that the peak observed at m/z 2975 ($[M + 16 + Na]^+$) in the $CHCl_3$ extract of Sample C completely disappeared, and only the peak at m/z 2959 ($[M + Na]^+$) was measured in the reduced sample (Figure S5, Supporting Information). This result clearly indicates that the peak at m/z 2975 is ascribed to the sulfoxidized Py3CD (abbreviated as Py3CD-O). The experiments using ^{18}O-labeled CHPO demonstrated that the oxygen atom of Py3CD-O came from O=Fe^{IV}PCD (Figure 6c,d).

Despite the fact that O=Fe^{IV}PCD in Sample B was completely consumed during 1 h and no O=Fe^{IV}PCD remained in Sample C, the peak of $[M + Na]^+$ was still observed with the same intensity as that of $[M + 16 + Na]^+$ (Figure 6b). Such a result is consistent with the result obtained from the UV–vis spectral measurements showing that half of the O=Fe^{IV}PCD molecules in Sample B were sulfoxidized and the rest returned to HO-Fe^{III}PCD (met-hemoCD, vide supra).

HPLC chromatograms of Samples B and C are shown in Figure 8. The main peak (Peak 2) of Sample B was ascribed to Py3CD, and small peaks from Py3CD-O (Peak 1) and demethylated Py3CD (Peak 3) were also observed. The chromatogram of Sample C indicates that half of the Py3CD molecules were sulfoxidized in spontaneous reaction of O=Fe^{IV}PCD. Such a result is in good agreement with that obtained

dx.doi.org/10.1021/ic4026393 | Inorg. Chem. 2014, 53, 543–551

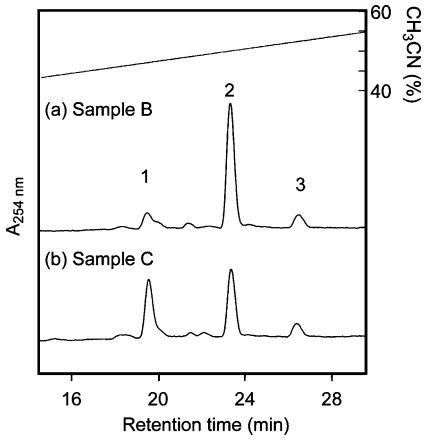

Figure 8. HPLC chromatograms of the $CHCl_3$ extract of Sample B (a) and Sample C (b). Each sample was eluted at a flow rate of 0.5 mL min^{-1} using H_2O-CH_3CN linear gradient (0.1% TFA). HPLC traces were monitored at 254 nm. Eluted fractions were analyzed by ESI-TOF MS and/or MALDI-TOF MS; Fraction 1: Py3CD-O, Fraction 2: Py3CD, Fraction 3: demethylated Py3CD.

from UV–vis spectral measurements, which show that O_2-Fe^{II}PCD-O and met-hemoCD are formed in a 1:1 ratio in a spontaneous reaction of O=Fe^{IV}PCD (vide supra). Therefore, it can be concluded that O_2-Fe^{II}PCD-O is the concomitant product of the two-electron oxidation of the sulfide bond, while the monohydroxo complex of met-hemoCD (HO-Fe^{III}PCD) is produced by a one-electron reduction of O=Fe^{IV}PCD with its surroundings. The detailed mechanism of the reduction of O=Fe^{IV}PCD to met-hemoCD remains unclear, while we knew that the addition of a small amount of acetonitrile (10%) into a Sample B solution induced an immediate conversion of O=Fe^{IV}PCD to met-hemoCD without intramolecular sulfoxidation.

The first-order rate constants for the intramolecular sulfoxidation of O=Fe^{IV}PCD were determined by measuring HPLC of the $CHCl_3$ extracts from the reaction mixtures of Sample B (Figure 9a). Figure 9b shows that the rate constant is

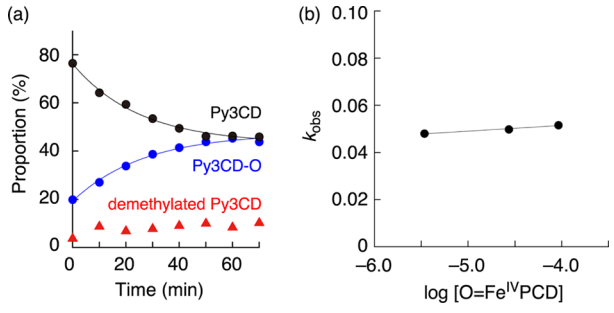

Figure 9. Time courses of the $CHCl_3$ extracts for the spontaneous reaction of Sample B (3.4×10^{-6} M) followed by HPLC (a) and the plot of the first-order rate constant (k_{obs}) for the formation of Py3CD-O versus [O=Fe^{IV}PCD] (b). The solid lines in panel a are the theoretical curves for the first-order kinetics.

independent of the initial concentration of O=Fe^{IV}PCD, indicating that no intermolecular sulfoxidation occurred in the present system. In addition, the disproportionation of O=Fe^{IV}PCD generating O=Fe^{IV}PCD$^{\bullet+}$ can be excluded from the reaction mechanism. Figure 9a suggests that the demethylation of Py3CD proceeded during the reaction producing Sample B, and no appreciable demethylation occurred during the spontaneous reaction of Sample B to give Sample C. The demethylation likely took place during the reaction of met-hemoCD with CHPO through a more active oxoferryl porphyrin cation radical (O=Fe^{IV}PCD$^{\bullet+}$) as exhibited in Scheme 3.[37] The formation of O=Fe^{IV}PCD$^{\bullet+}$ seems to be quite slight compared with that of O=Fe^{IV}PCD in the reaction of met-hemoCD with H_2O_2 or CHPO.

Scheme 3

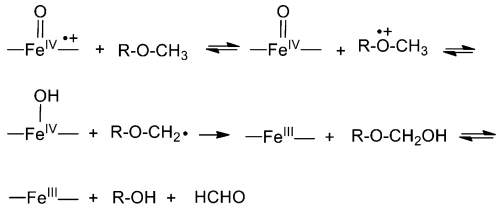

Structures of O=Fe^{IV}PCD. One of the plausible structures of O=Fe^{IV}PCD (Structure A) is shown in Figure 10, where

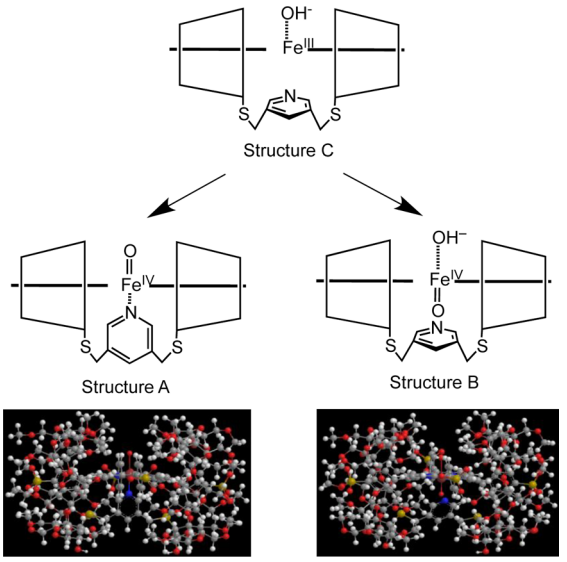

Figure 10. Plausible structures of O=Fe^{IV}(Py)PCD (Structure A) and O=Fe^{IV}(OH^-)PCD (Structure B) and their precursor (Structures C). The structures shown in the bottom were obtained from the MM3 calculations.

iron-oxo oxygen is located on the other side of the sulfide bonds of Py3CD across a porphyrin surface. Under such circumstances, no sulfoxidation occurs because the porphyrin ring cannot rotate freely owing to steric interference between the sulfonatophenyl groups at the meso-positions of FeTPPS and the linker of Py3CD. Another probable structure is shown to be Structure B in Figure 10, whose iron-oxo oxygen is located on the same side as the sulfide bonds. The MM3 calculations suggest that Structure B is sterically reasonable, as is Structure A. The pK_a of the axial H_2O of met-hemoCD is 5.5.[28] In phosphate buffer at pH 7.0, the axial ligand of met-hemoCD is the electron-donating hydroxo ligand leading to a weakening of the pyridine–Fe^{III} bond.

The formation of Structure C in a five-coordinate high-spin state was supported by an intense EPR signal at g = 6.03 for met-hemoCD in a phosphate buffer at 15 K (Supporting Information, Figure S6). ^{1}H NMR spectrum of met-hemoCD

dx.doi.org/10.1021/ic4026393 | Inorg. Chem. 2014, 53, 543–551

Scheme 4

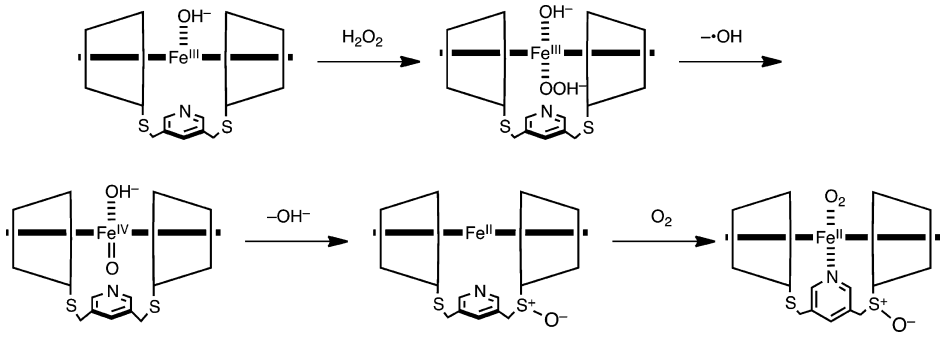

in D_2O at pD 7.0 showed a signal from the pyrrole β-protons as a broad singlet at 83 ppm (Figure S7, Supporting Information), supporting the formation of a five-coordinate high-spin state (Structure C).[25b,38] Structure C seems to be the common intermediate yielding HOO-Fe^{III}(OH^-) and HOO-Fe^{III}(Py)-PCD. We previously reported an EPR spectrum composed of two sets of rhombic signals ($g_{1,2,3}$ = 2.24, 2.14, 1.96; $g'_{1,2,3}$ = 2.22, 2.12, 1.97) at 15 K for a sample obtained by freezing the met-hemoCD solution immediately after the addition of H_2O_2.[26] These two sets of the rhombic signals were assigned to HOO-Fe^{III}(OH^-)PCD and HOO-Fe^{III}(Py)PCD. Tajima et al. reported the EPR spectra of the hydroperoxo complexes of Fe^{III}TMP, the axial ligands of which were hydroxo (HOO-Fe^{III}(OH^-)TMP, g = 2.257, 2.156, 1.963) and imidazole (HOO-Fe^{III}(Im)TMP, g = 2.320, 2.191, 1.943), in a DMF/methanol/toluene/H_2O mixed solvent at −60 °C.[39] The same research group also reported the EPR spectrum of HOO-Fe^{III}(pyridine)OEP (OEP: octaethylporphyrin dianion) with g = 2.28, 2.17, and 1.95.[40] The results obtained by Tajima et al. suggest that the rhombic signal with g values at 2.22, 2.12, and 1.97 is ascribed to HOO-Fe^{III}(OH^-)PCD. The slightly weaker rhombic signal with g values at 2.24, 2.14, and 1.96 seems to be attributable to HOO-Fe^{III}(Py)PCD. O=Fe^{IV}(OH^-)PCD produced from HOO-Fe^{III}(OH^-)PCD may transfer its oxo oxygen to the sulfide bond. Meanwhile, O=Fe^{IV}(Py)PCD formed via HOO-Fe^{III}(Py)PCD seems to be reduced by its surroundings affording met-hemoCD. The spontaneous reaction of O=Fe^{IV}PCD, which was the product of the reaction of met-hemoCD with H_2O_2 at pH 5.0, in a phosphate buffer at pH 5.0 gave 15% of O_2-Fe^{II}PCD and 85% of H_2O-Fe^{III}PCD (see Figure S8, Supporting Information). Such a result supports our assumption that both O=Fe^{IV}(Py)PCD and O=Fe^{IV}(OH^-)PCD are formed in the reaction of met-hemoCD with H_2O_2 or CHPO at pH 7.0.

CONCLUSION

A 1:1 inclusion complex (met-hemoCD) of Fe^{III}TPPS and Py3CD rapidly reacted with H_2O_2 to form two types of stable oxoferryl complexes (O=Fe^{IV}(OH^-)PCD and O=Fe^{IV}(Py)-PCD), through a homolysis of their precursors, HOO-Fe^{IV}(OH^-)PCD and HOO-Fe^{IV}(Py)PCD, respectively. Despite the hydroxyl radical causing a ring-opening reaction of FeTPPS in the absence of Py3CD, no appreciable decomposition of the porphyrin ring occurred in the reaction of met-hemoCD with H_2O_2. The hydroxyl radical was stabilized in a Py3CD capsule through the equilibrium [HOO-Fe^{IV}PCD ⇄ O=Fe^{IV}PCD + •OH]. O=Fe^{IV}PCDs were stable enough that such high-valent oxo complexes could be chromatographically separated from the oxidant such as H_2O_2 or CHPO. The spontaneous reaction of O=Fe^{IV}(OH^-)PCD affords O_2-Fe^{II}PCD-O, whose Py3CD component was sulfoxidized through the direct intramolecular oxygen transfer of the oxo oxygen to the sulfide bond of Py3CD (Scheme 4). Meanwhile, O=Fe^{IV}(Py)PCD was reduced to met-hemoCD (HO-Fe^{III}(Py)PCD) with its surroundings without any transformation of its cyclodextrin component. The present study also suggested the occurrence of competitive formation of a small amount of O=$Fe^{IV}$$PCD^{•+}$ in the reaction of met-hemoCD with CHPO. O=$Fe^{IV}$$PCD^{•+}$ was active enough that it caused the demethylation of an OCH_3 group of Py3CD through the hydroxylation giving an acetal (Scheme 3). The Py3CD provided a unique capsule and/or a cage to Fe^{III}TPPS. The cage effect on equilibrium, HOO−Fe^{III}PCD ⇄ O=Fe^{IV}PCD + •OH, made it possible to inactivate hydroxyl radical. Detection of O_2-Fe^{II}PCD-O in the spontaneous reaction of O=Fe^{IV}(OH^-)PCD was also achieved by the cage effect of the cyclodextrin dimer that prohibited the escape of dioxygen dissociated from the iron center.[27,28] Cyclodextrin dimer/metal porphyrin systems may be useful for investigating models of metal enzymes.

We also studied the intermolecular reactions of O=Fe^{IV}PCD with thioanisole and guaiacol. A quantitative one-electron oxidation of guaiacol was observed (see Figure S9, Supporting Information), while thioanisole did not react with O=Fe^{IV}PCD. Masking of the iron center by the two cyclodextrin cavities may inhibit intermolecular direct oxygen transfer from O=Fe^{IV}PCD to thioanisole.

ASSOCIATED CONTENT

Supporting Information

Rates of formation of O=Fe^{IV}PCD in the reactions of met-hemoCD with H_2O_2, UV−vis spectral changes during the reaction of uncomplexed Fe^{III}TPPS with H_2O_2, HPLC chromatogram of the ring-opening products of Fe^{III}TPPS, gel-filtration trace of Sample A, MALDI-TOF mass spectrum of the reaction mixture obtained by reduction of the $CHCl_3$ extract of Sample C with Mg/methanol, EPR spectrum of met-hemoCD, ^1H NMR spectrum of met-hemoCD, UV−vis spectral changes during the spontaneous reaction of O=Fe^{IV}PCD at pH 5.0 and UV−vis spectra of the reaction product under a CO atmosphere, and UV−vis spectral changes during the reaction of O=Fe^{IV}PCD with guaiacol. This material is available free of charge via the Internet at http://pubs.acs.org.

AUTHOR INFORMATION

Corresponding Author

*E-mail: kkano@mail.doshisha.ac.jp.

dx.doi.org/10.1021/ic4026393 | Inorg. Chem. 2014, 53, 543−551

Notes

The authors declare no competing financial interest.

■ ACKNOWLEDGMENTS

This study was supported by Grants-in-Aid on Construction of Research Base in Private University from the Ministry of Education, Sports, Science and Technology.

■ REFERENCES

(1) (a) Denisov, I. G.; Makris, T. M.; Sligar, S. G.; Schlichting, I. *Chem. Rev.* **2005**, *105*, 2253−2278. (b) Ortiz de Montellano, P. R. *Chem. Rev.* **2010**, *110*, 932−948. (c) Fukuzumi, S. *Coord. Chem. Rev.* **2013**, *257*, 1564−1575. (d) Lane, B. S.; Burgess, K. *Chem. Rev.* **2003**, *103*, 2457−2474. (e) Sono, M.; Roach, M. P.; Coulter, E. D.; Dawson, J. H. *Chem. Rev.* **1996**, *96*, 2841−2888.

(2) (a) Rydberg, P.; Sigfridsson, E.; Ryde, U. *J. Biol. Inorg. Chem.* **2004**, *9*, 203−223. (b) Ling, K.-Q.; Li, W.-S.; Sayre, L. M. *J. Am. Chem. Soc.* **2008**, *130*, 933−944.

(3) (a) Kumar, D.; Karamzadeh, B.; Sastry, G. N.; de Visser, S. P. *J. Am. Chem. Soc.* **2010**, *132*, 7656−7667. (b) Meunier, B.; de Visser, S. P.; Shaik, S. *Chem. Rev.* **2004**, *104*, 3947−3980.

(4) Goto, Y.; Matsui, T.; Ozaki, S.; Watanabe, Y.; Fukuzumi, S. *J. Am. Chem. Soc.* **1999**, *121*, 9497−9502.

(5) (a) Kobayashi, S.; Nakano, M.; Kimura, T.; Schaap, A. P. *Biochemistry* **1987**, *26*, 5019−5022. (b) Dawson, J. H. *Science* **1988**, *240*, 433−439. (c) Baciocchi, E.; Lanzalunga, O.; Malandrucco, S.; Ioele, M.; Steenken, S. *J. Am. Chem. Soc.* **1996**, *118*, 8973−8974. (d) Nam, W. *Acc. Chem. Res.* **2007**, *40*, 522−531.

(6) Watanabe, Y.; Numata, T.; Iyanagi, T.; Oae, S. *Bull. Chem. Soc. Jpn.* **1981**, *54*, 1163−1170.

(7) (a) Li, C.; Zhang, L.; Zhang, C.; Hirao, H.; Wu, W.; Shaik, S. *Angew. Chem., Int. Ed.* **2007**, *46*, 8168−8170. (b) Cho, K. B.; Moreau, Y.; Kumar, D.; Rock, D. A.; Jones, J. P.; Shaik, S. *Chem.—Eur. J.* **2007**, *13*, 4103−4115. (c) Shaik, S.; Wang, Y.; Chen, H.; Song, J.; Meir, R. *Faraday Discuss.* **2010**, *145*, 49−70.

(8) Peñéñory, A. B.; Argüello, J. E.; Puiatti, M. *Eur. J. Org. Chem.* **2005**, *2005*, 114−122.

(9) Matsui, T.; Kim, S. H.; Jin, H.; Hoffman, B. M.; Ikeda-Saito, M. *J. Am. Chem. Soc.* **2006**, *128*, 1090−1091.

(10) Harris, R. Z.; Newmyer, S. L.; Ortiz de Montellano, P. R. *J. Biol. Chem.* **1993**, *268*, 1637−1645.

(11) Rydberg, P.; Jørgensen, M. S.; Jacobsen, T. A.; Jacobsen, A.-M.; Madsen, K. G.; Olsen, L. *Angew. Chem., Int. Ed.* **2013**, *52*, 993−997.

(12) (a) Kedderis, G. L.; Rickert, D. E.; Pandey, R. N.; Hollenberg, P. F. *J. Biol. Chem.* **1986**, *261*, 15910−15914. (b) Ortiz de Montellano, P. R.; Choe, Y. S.; DePillis, G.; Catalano, C. E. *J. Biol. Chem.* **1987**, *262*, 11641−11646.

(13) Hessenauer-Ilicheva, N.; Franke, A.; Meyer, D.; Woggon, W.-D.; van Eldik, R. *J. Am. Chem. Soc.* **2007**, *129*, 12473−12479.

(14) Han, A.-R.; Jeong, Y. J.; Kang, Y.; Lee, J. Y.; Seo, M. S.; Nam, W. *Chem. Commun.* **2008**, 1076−1078.

(15) Bell, S. R.; Groves, J. T. *J. Am. Chem. Soc.* **2009**, *131*, 9640−9641.

(16) Chiavarino, B.; Cipollini, R.; Crestoni, M. E.; Fornarini, S.; Lanucara, F.; Lapi, A. *J. Am. Chem. Soc.* **2008**, *130*, 3208−3217.

(17) Takahashi, A.; Kurahashi, T.; Fujii, H. *Inorg. Chem.* **2009**, *48*, 2614−2625.

(18) Chin, D.-H.; La Mar, G. N.; Balch, A. L. *J. Am. Chem. Soc.* **1980**, *102*, 5945−5947.

(19) Groves, J. T.; Gross, Z.; Stern, M. K. *Inorg. Chem.* **1994**, *33*, 5065−5072.

(20) Nam, W.; Park, S.; Lim, I. K.; Lim, M. H.; Hong, J.; Kim, J. *J. Am. Chem. Soc.* **2003**, *125*, 14674−14675.

(21) Nehru, K.; Seo, M. S.; Kim, J.; Nam, W. *Inorg. Chem.* **2006**, *46*, 293−298.

(22) Jeong, Y. J.; Kang, Y.; Han, A.-R.; Lee, Y.-M.; Kotani, H.; Fukuzumi, S.; Nam, W. *Angew. Chem., Int. Ed.* **2008**, *47*, 7321−7324.

(23) Fertinger, C.; Hessenauer-Ilicheva, N.; Franke, A.; van Eldik, R. *Chem.—Eur. J.* **2009**, *15*, 13435−13440.

(24) Pan, Z.; Newcomb, M. *Inorg. Chem.* **2007**, *46*, 6767−6774.

(25) (a) Keilin, D.; Hartree, E. F. *Biochem. J.* **1951**, *49*, 88−106. (b) Adediran, S. A.; Lambeir, A.-M. *Eur. J. Biochem.* **1989**, *186*, 571−576.

(26) Kitagishi, H.; Tamaki, M.; Ueda, T.; Hirota, S.; Ohta, T.; Naruta, Y.; Kano, K. *J. Am. Chem. Soc.* **2010**, *132*, 16730−16732.

(27) (a) Kano, K.; Kitagishi, H.; Kodera, M.; Hirota, S. *Angew. Chem., Int. Ed.* **2005**, *44*, 435−438. (b) Kano, K.; Kitagishi, H.; Dagallier, C.; Kodera, M.; Matsuo, T.; Hayashi, T.; Hisaeda, Y.; Hirota, S. *Inorg. Chem.* **2006**, *45*, 4448−4460.

(28) Kano, K.; Chimoto, S.; Tamaki, M.; Itoh, Y.; Kitagishi, H. *Dalton Trans.* **2012**, *41*, 453−461.

(29) Lente, G.; Fabian, I. *Dalton Trans.* **2007**, 4268−4275.

(30) Kano, K.; Kitagishi, H.; Tamura, S.; Yamada, A. *J. Am. Chem. Soc.* **2004**, *126*, 15202−15210.

(31) Ueda, T.; Kitagishi, H.; Kano, K. *Org. Biomol. Chem.* **2012**, *10*, 4337−4347.

(32) Finn, M. G.; Sharpless, K. B. *J. Am. Chem. Soc.* **1991**, *113*, 113−126.

(33) (a) Derat, E.; Kumar, D.; Hirao, H.; Shaik, S. *J. Am. Chem. Soc.* **2006**, *128*, 473−484. (b) Chen, H.; Moreau, Y.; Derat, E.; Shaik, S. *J. Am. Chem. Soc.* **2008**, *130*, 1953−1965.

(34) Lawrence, A.; Jones, C. M.; Wardman, P.; Burkitt, M. J. *J. Biol. Chem.* **2003**, *278*, 29410−29419.

(35) Scheidt, W. R.; Reed, C. A. *Chem. Rev.* **1981**, *81*, 543−555.

(36) Khurana, J. M.; Sharma, V.; Chacko, S. A. *Tetrahedron* **2007**, *63*, 966−969.

(37) Ueda, T.; Kumeda, S.; Kitagishi, H.; Kano, K. *Chem. Lett.* **2013**, *42*, 1366−1368.

(38) (a) Keilin, D.; Mann, T. *Proc. R. Soc. London, Ser. B* **1937**, *122* (827), 119−133. (b) Tuynman, A.; Schoemaker, H. E.; Wever, R. *Monatsh. Chem.* **2000**, *131*, 687−695.

(39) Tajima, K.; Oka, S.; Edo, T.; Miyake, S.; Mano, H.; Mukai, K.; Sakurai, H.; Ishizu, K. *J. Chem. Soc., Chem. Commun.* **1995**, 1507−1508.

(40) Tajima, K.; Shigematsu, M.; Jinno, J.; Ishizu, K.; Ohya-Nishiguchi, H. *J. Chem. Soc., Chem. Commun.* **1990**, 144−145.